Estimating aquifer hydraulic properties using sinusoidal pumping at the Savannah River site, South Carolina, USA

Todd C. Rasmussen · Kevin G. Haborak · Michael H. Young

Abstract A framework for estimating aquifer hydraulic properties using sinusoidal pumping is presented that (1) derives analytical solutions for confined, leaky, and partially penetrating conditions; (2) compares the analytical solutions with a finite element model; (3) establishes a field protocol for conducting sinusoidal aquifer tests; and (4) estimates aquifer parameters using the analytical solutions. The procedure is demonstrated in one surficial and two confined aquifers containing potentially contaminated water in coastal plain sediments at the Savannah River site, a federal nuclear facility. The analytical solutions compare favorably with finite-element solutions, except immediately adjacent to the pumping well where the assumption of zero borehole radius is not valid. Estimated aquifer properties are consistent with previous studies for the two confined aquifers, but are inconsistent for the surficial aquifer; conventional tests yielded estimates of the specific yield—consistent with an unconfined response—while the shorter-duration sinusoidal perturbations yielded estimates of the storativity—consistent with a confined, elastic response. The approach minimizes investigation-derived wastes, a significant concern where contaminated fluids must be disposed of in an environmentally acceptable manner. An additional advantage is the ability to introduce a signal different from background perturbations, thus easing detection.

01 Tanmoy Das

02 Tanmoy Das

03 Tanmoy Das

Received: 16 August 2002 / Accepted: 13 February 2003
Published online: 24 April 2003

T. C. Rasmussen (✉)
School of Forest Resources, University of Georgia,
1040 D.W. Brooks Drive, Athens, Georgia, 30602-2152, USA
e-mail: trasmuss@uga.edu
Tel.: +1-706-5424300
Fax: +1-706-5428356

K. G. Haborak
Golder International, 3730 Chamblee Tucker Road,
Atlanta, Georgia, 30341, USA

M. H. Young
Division of Hydrologic Sciences, Desert Research Institute,
755 E. Flamingo Road, Las Vegas, Nevada, 89119, USA

Résumé Une démarche pour estimer les propriétés d'un aquifère à partir d'un débit de pompage à variations sinusoïdales est présentée pour (1) dériver des solutions analytiques pour des conditions captives, en drainance, et de puits incomplet convenant à plusieurs applications pratiques, (2) vérifier les solutions analytiques par rapport à un modèle aux éléments finis, (3) établir un protocole de terrain pour réaliser des essais d'aquifère, et (4) estimer les paramètres de l'aquifère à partir de solutions analytiques. Les solutions analytiques soutiennent bien la comparaison avec les solutions aux éléments finis d'un domaine d'écoulement simulé, sauf dans les zones immédiatement voisines du puits de pompage où l'hypothèse d'un rayon de forage nul n'est pas respectée. La procédure de terrain utilise (1) une chaîne d'acquisition de données programmable que contrôlent des pompes à régime variable qui alternativement injectent et extraient l'eau du forage pour créer une impulsion sinusoïdale, (2) un conteneur mobile, au-dessus du sol qui stocke momentanément l'eau de l'aquifère entre les cycles d'extraction et d'injection, (3) des débitmètres à palettes qui contrôlent les débits d'extraction et d'injection, et (4) des capteurs de pression qui contrôlent les niveaux d'eau dans les forages de pompage et d'observation. La procédure est appliquée à une unité aquifère superficielle et à deux unités captives du site de la rivière Savannah, un site nucléaire fédéral de Caroline du Sud. L'approche sinusoïdale fournit rapidement des estimations des paramètres de l'aquifère en évitant les pertes de temps liées aux études.

Resumen Se presenta un marco para estimar las propiedades de los acuíferos mediante una tasa de extracción sinusoidal. El método (1) deriva soluciones analíticas para condiciones de acuífero confinado, semiconfinado y de penetración parcial, que son aplicables a muchas situaciones prácticas; (2) verifica las soluciones analíticas con un modelo de elementos finitos; (3) establece un protocolo de campo para ejecutar ensayos hidráulicos; y (4) estima los parámetros del acuífero por medio de las soluciones analíticas. Éstas han sido validadas de forma satisfactoria con soluciones numéricas en un dominio simulado de flujo, exceptuando las áreas adyacentes al pozo de bombeo, para el que la hipótesis de radio nulo no se cumple. El procedimiento de campo utiliza (1) un registrador de datos programable que controla las bombas

 DOI 10.1007/s10040-003-0255-7

de velocidad variable que inyectan y extraen agua de forma alternativa desde el sondeo con el fin de crear un estímulo sinusoidal; (2) un contenedor móvil, situado en superficie, que almacena temporalmente el fluido del acuífero durante los ciclos; (3) contadores volumétricos tipo noria que registran las tasas de inyección y extracción; y (4) transductores de presión para observar los niveles del agua en los sondeos de bombeo y control. El procedimiento ha sido verificado en un acuífero superficial y en dos niveles confinados del emplazamiento del río Savannah, en Carolina del Sur (Estados Unidos de América), donde se ubican unas instalaciones nucleares federales. El enfoque sinusoidal permite efectuar estimaciones rápidas de los parámetros del acuífero a la par que elimina residuos derivados de la investigación.

Keywords Equipment · Field techniques · Hydraulic testing · Groundwater hydraulics · Hydraulic properties · Sinusoidal testing

Introduction

Site characterization at locations with contaminated groundwater require hydraulic testing to determine aquifer hydraulic properties, primarily the aquifer transmissivity, storativity, and leakage coefficient. Conventional aquifer tests rely on constant extraction of water from, or injection into, a well bore with contemporaneous monitoring of observation wells. The measured response in the observation wells is then used to estimate aquifer hydraulic properties.

Aquifer tests that rely on groundwater pumping often generate substantial volumes of water, which may be contaminated with hazardous chemicals. Due to potential contamination of these investigation-derived wastes, the water may need to be collected, stored, treated, and disposed of in an environmentally responsible manner at substantial costs.

A sinusoidal excitation of fluid pressure within the pumping borehole is an alternative method for aquifer testing. Advantages of the sinusoidal approach compared to the constant flow aquifer test are: (1) investigation-derived wastes are eliminated, thus reducing disposal costs for contaminated water, (2) the oscillating signal of known frequency is separable from changing background pressure, (3) the time required to achieve steady conditions is shorter, and (4) it is theoretically possible to perform multiple tests simultaneously using unique frequencies for each of the source boreholes. Disadvantages of a sinusoidal test include: (1) measurable signals may not propagate as far into the aquifer as those from the constant flow method, (2) there have been few published methods of interpreting data from sinusoidal tests, and (3) more complex field instruments and pump controllers are needed to conduct the aquifer test.

04 Tanmoy Das

05 Tanmoy Das

A sinusoidal pressure signal can be created with a fixed period and amplitude. The pressure wave created by this excitation diffuses into the aquifer and attenuates as it diffuses. Observation boreholes are used to detect the amplitude attenuation and phase lag of the signal. The attenuation and phase lag of the signal depend on the distance of the observation boreholes from the pumping borehole, the frequency of the sinusoidal excitation, and the aquifer hydraulic properties.

06 Tanmoy Das

The purpose of this paper is to present analytical solutions for sinusoidal aquifer tests, and to demonstrate the feasibility of the approach in three coastal-plain aquifers at the Savannah River site. Sinusoidal aquifer test solutions are presented for confined (Theis 1935) and leaky (Hantush and Jacob 1955) aquifers for wells that fully penetrate the aquifer, along with an analytic solution for confined aquifers with partially penetrating wells (Hantush 1964). A numerical model is compared to the analytical solutions to evaluate the adequacy of the approach. Finally, field test equipment is used to demonstrate the feasibility of the technique for a test well complex at the Savannah River site. Interpretation of the sinusoidal aquifer test data is then provided using field data from the Savannah River site.

Background

An early method for determining aquifer hydraulic properties for sinusoidal inputs was presented by Ferris (1963). This approach yields an estimate of aquifer transmissivity for a sinusoidal tidal input to a confined, one-dimensional (horizontal, x) flow domain. Gelhar (1974) presented the response in an aquifer to sinusoidal perturbations using three types of aquifer models: a linear reservoir model, a linear Dupuit aquifer, and a Laplace aquifer. Flow in the first two cases occurs in a single horizontal, x, dimension, while the Laplace aquifer also includes a vertical flow dimension, z. The form of these solutions precludes their use for interpreting radial flow to a borehole, r.

Black and Kipp (1981) were the first to provide a solution to an aquifer borehole test for a sinusoidal perturbation in a confined non-leaky aquifer. Solutions are provided for both a point source (a well screened over a very small section relative to the entire thickness of an aquifer) and a line source (a well screened over the entire thickness of the aquifer). The approach uses the ratio of either the phase shift or amplitude from two observation wells to determine the aquifer hydraulic diffusivity. Unfortunately, their method does not provide the ability to independently determine both the aquifer transmissivity and storativity coefficient.

Natural excitations (such as precipitation, evapotranspiration, barometric pressure, and tidal fluctuations) often show periodic behavior, making it possible to use sinusoidal analysis to determine aquifer hydraulic properties. Approaches that use naturally occurring excitations to estimate subsurface properties include barometric pressure perturbations (Rojstaczer 1988; Rojstaczer and Riley 1990; Rasmussen and Crawford 1997; Mehnert et al. 1999) as well as earth tide perturbations (Hsieh et al.

 DOI 10.1007/s10040-003-0255-7

1987; Ritzi et al. 1991). These approaches take advantage of naturally occurring perturbations as the stimulus, and then estimate aquifer properties using the observed response in a borehole. The magnitude of natural excitations is normally much smaller than those induced during aquifer tests.

One drawback of using natural excitations is the complexity of natural system behavior, often being a mixture of processes including: (1) vertical transmission of the barometric pressure stimulus through the unsaturated zone in the case of surficial aquifers, (2) vertical transmission of surface loads through overlying units in confined aquifers, (3) horizontal propagation within the monitored aquifer, and (4) borehole storage responses. Two advantages, therefore, of induced sinusoidal stimulation are that the system geometry can be simplified by removing the vertical propagation from the earth's surface, and that a single frequency can be specified for excitation.

Analytical Solutions

Analytical solutions are presented for sinusoidal equivalents of three steady-flow aquifer testing conditions: (1) the Theis (1935) solution of the confined aquifer problem, (2) the Hantush and Jacob (1955) solution of the leaky aquifer problem, and (3) the Hantush (1964) solution for a partially penetrating pumping well. The assumptions in these models are that the aquifer is homogeneous, uniform in thickness, compressible and elastic, horizontal, and of infinite areal extent; groundwater flow is described by Darcy's law; pore fluids are elastic and of constant density and viscosity; the initial piezometric surface is horizontal; the pumping well has an infinitesimal diameter; head losses through the well screen are negligible; and the pumping rate is constant.

Confined Aquifer Solution

Theis (1935) introduced an analytical solution for a well pumping at a constant rate from a confined aquifer system. The additional assumptions in the Theis solution are that the aquifer is isotropic; groundwater flow is horizontal; and the pumping well is fully penetrating. Black and Kipp (1981) introduced an analytical solution for a well pumping sinusoidally in a confined aquifer system. The assumptions in this solution are identical to those of the Theis solution with the exception of the pumping rate being sinusoidal. For the derivation of the solution to the boundary value problem, the complex exponential function will be used to represent the sinusoidal pumping rate. The value of the complex exponential function is given by:

$$Q_o\, e^{\mathbf{i}\omega t} = Q_o\, [\cos \omega t + \mathbf{i} \sin \omega t] \tag{1}$$

where Q is the complex pumping rate, Q_o is the amplitude of the pumping rate, ω is the frequency of the excitation, t is a time variable, and i is the imaginary number. Using this representation has the advantage that the final solution includes the response to both the real and imaginary components of the sinusoidal pumping rate. The final solution is a complex-valued function where the real part is the response to the real component of the pumping rate and the imaginary part is the response to the imaginary component of the pumping rate (Saff and Snider 1993). Thus, the boundary value problem can be stated mathematically using:

$$\frac{\partial^2 s}{\partial r^2} + \frac{1}{r}\frac{\partial s}{\partial r} = \frac{1}{D}\frac{\partial s}{\partial t} \tag{2}$$

$$s(r, 0) = 0 \tag{3}$$

$$s(\infty, t) = 0 \tag{4}$$

$$\lim_{r \to 0} r \frac{\partial s}{\partial r} = \frac{Q}{2\pi T} \tag{5}$$

where D is the hydraulic diffusivity, s is the observed drawdown, r is the distance from the pumping well, and T is the aquifer transmissivity. The solution to this problem, derived in the Appendix, yields the steady periodic response to a sinusoidal pumping rate:

$$s(r, t) = \frac{Q}{2\pi T} K_o\left(r\sqrt{\frac{\mathbf{i}\omega}{D}}\right) \tag{6}$$

where K_o is the zero-order modified Bessel function of the second kind. This solution neglects a nonperiodic, initial-transient component that decays with time after the beginning of the sinusoidal aquifer test.

The amplitude of the water level fluctuations in an observation well is:

$$|s| = \frac{Q_o}{2\pi T}\left|K_o\left(r\sqrt{\frac{\mathbf{i}w}{D}}\right)\right| \tag{7}$$

and the phase shift, ϕ, is:

$$\phi = arg\left\{K_o\left(r\sqrt{\frac{\mathbf{i}w}{D}}\right)\right\} \tag{8}$$

This result is consistent with solution 215.08 in Bruggeman (1999). These results are different in form but consistent with the Black and Kipp (1981) solution. The results presented here are different because the Black and Kipp solution employs a sinusoidal drawdown for the excitation boundary instead of a sinusoidal flux boundary condition. Introducing the flux boundary conditions provides the ability to estimate both the transmissivity and storativity using Eqs. (7) and (8). Barker (1988) presented an alternative Laplace transform solution approach to this problem.

Leaky Aquifer Solution

Hantush and Jacob (1955) derived an analytical solution for a well pumping constantly from a leaky aquifer system. The solution is appropriate for an aquifer that is bounded above or below by an aquiclude and bounded on

 DOI 10.1007/s10040-003-0255-7

the opposing surface by an aquitard and a source aquifer. The additional assumptions in the Hantush and Jacob solution are that the hydraulic conductivity of the aquitard is so small relative to the aquifers that flow in this layer is essentially vertical; the aquitard is incompressible; and the water table in the source bed is horizontal and remains constant (therefore, the rate of leakage from the aquitard into the pumped aquifer is directly proportional to the drawdown at the interface).

The assumptions are identical to the Hantush and Jacob assumptions, with the exception that the pumping rate is sinusoidal:

$$\frac{\partial^2 s}{\partial r^2} + \frac{1}{r}\frac{\partial s}{\partial r} - \frac{s}{B^2} = \frac{1}{D}\frac{\partial s}{\partial t} \tag{9}$$

$$s(r,0) = 0 \tag{10}$$

$$s(\infty, t) = 0 \tag{11}$$

$$\lim_{r\to 0} r\frac{\partial s}{\partial r} = -\frac{Q}{2\pi T} \tag{12}$$

and where

$$B^2 = \frac{T}{L} = \frac{T m'}{K'} \tag{13}$$

where $L=K'/m'$ is the aquifer leakance, and m' and K' are the thickness and vertical hydraulic conductivity of the confining layer, respectively. The steady periodic response to sinusoidal pumping in a leaky aquifer, as derived in the Appendix, is:

$$s(r,t) = \frac{Q}{2\pi T} K_o\left(r\sqrt{\frac{\mathbf{i}\omega}{D} + \frac{1}{B^2}}\right) \tag{14}$$

where the nonperiodic, initial-transient response is neglected.

The amplitude of the water level response in an observation well is:

$$|s| = \frac{Q_o}{2\pi T}\left|K_o\left(r\sqrt{\frac{\mathbf{i}\omega}{D} + \frac{1}{B^2}}\right)\right| \tag{15}$$

and the phase shift is:

$$\phi = arg\left\{K_o\left(r\sqrt{\frac{\mathbf{i}\omega}{D} + \frac{1}{B^2}}\right)\right\} \tag{16}$$

The result is consistent with Solution 215.18 in Bruggeman (1999), except for a factor of two errors in the Bruggeman solution, i.e., the denominator in Bruggeman should be $2\pi T$ instead of $4\pi T$.

Partially Penetrating Well Solution

Hantush (1964) presented a solution for a partially penetrating well pumping from a confined aquifer. The solution is appropriate for an aquifer bounded above and below by aquicludes. The additional assumptions in the Hantush solution are that the aquifer is anisotropic; the pumping well is partially penetrating (screened) from d to l; and the observation well is screened over the interval from d' to l'.

The assumptions are identical except that it is assumed that the aquifer is isotropic and the pumping rate is sinusoidal. This boundary value problem is expressed mathematically as:

$$\frac{\partial^2 s}{\partial r^2} + \frac{1}{r}\frac{\partial s}{\partial r} + \frac{\partial^2 s}{\partial z^2} = \frac{1}{D}\frac{\partial s}{\partial t} \tag{17}$$

$$s(r, z, 0) = 0 \tag{18}$$

$$s(\infty, z, t) = 0 \tag{19}$$

$$\left.\frac{\partial s}{\partial z}\right|_{z=0} = 0 \tag{20}$$

$$\left.\frac{\partial s}{\partial z}\right|_{z=m} = 0 \tag{21}$$

$$\lim_{r\to 0} r\frac{\partial s}{\partial r} = \begin{cases} 0 & 0 \le z < d \\ -\frac{Q}{2\pi K(l-d)} & d \le z \le l \\ 0 & l < z \le m \end{cases} \tag{22}$$

where m is the aquifer thickness, K is the aquifer hydraulic conductivity, l and d are the upper and lower limits of the screened zone within the pumping well, respectively, and l' and d' are the upper and lower limits of the screened zone in the observation well, respectively. The steady periodic solution to sinusoidal pumping in a confined aquifer with a partially penetrating well, as derived in the Appendix, is:

$$s(r,l',d',t) = \frac{Q}{2\pi T}\left\{K_o\left(r\sqrt{\frac{\mathbf{i}\omega}{D}}\right) + \frac{2m^2}{\pi^2(l-d)(d'-l')}\sum_{n=1}^{\infty}\left\{\frac{1}{n^2}\left[\sin\frac{n\pi l}{m} - \sin\frac{n\pi d}{m}\right] K_o\left(r\sqrt{\frac{\mathbf{i}\omega}{D} + \left[\frac{n\pi}{m}\right]^2}\right)\left[\sin\frac{n\pi l'}{m} - \sin\frac{n\pi d'}{m}\right]\right\}\right) \tag{23}$$

where the nonperiodic, initial-transient components are again neglected. The amplitude of the water level response in an observation well is:

$$|s| = \frac{Q_o}{2\pi T}\left|K_o\left(r\sqrt{\frac{\mathbf{i}\omega}{D}}\right) + \frac{2m^2}{\pi^2(l-d)(d'-l')}\sum_{n=1}^{\infty}\left\{\frac{1}{n^2}\left[\sin\frac{n\pi l}{m} - \sin\frac{n\pi d}{m}\right] K_o\left(r\sqrt{\frac{\mathbf{i}\omega}{D} + \left[\frac{n\pi}{m}\right]^2}\right)\left[\sin\frac{n\pi l'}{m} - \sin\frac{n\pi d'}{m}\right]\right\}\right) \tag{24}$$

and the phase shift of the response is

 DOI 10.1007/s10040-003-0255-7

Table 1 Root-mean-squared differences between analytical solutions and finite-element simulation models, expressed as a percentage of the analytical solution

Time (h)	Nodes within 2 m of pumped well			Nodes beyond 2 m of pumped well		
	Confined aquifer	Leaky aquifer	Partially penetrating aquifer	Confined aquifer	Leaky aquifer	Partially penetrating aquifer
6	9.2	8.4	13.3	4.4	0.1	0.9
7.5	7.5	6.5	10.5	5.4	0.1	0.6
10	7.9	8.4	12.8	2.8	0.1	0.9
15	7.0	7.5	11.4	2.0	0.1	0.7
30	8.0	8.4	12.9	0.6	0.1	0.9

$$\phi = arg\left\{ K_o\left(r\sqrt{\frac{\mathbf{i}\omega}{D}}\right) + \frac{2m^2}{\pi^2(l-d)(d'-l')}\int_{n=1}^{\infty}\left\{\frac{1}{n^2}\left[sin\frac{n\pi l}{m} - sin\frac{n\pi d}{m}\right] K_o\left(r\sqrt{\frac{\mathbf{i}\omega}{D} + \left[\frac{n\pi}{m}\right]^2}\right)\left[sin\frac{n\pi l'}{m} - sin\frac{n\pi d'}{m}\right]\right)\right) \quad (25)$$

This solution has not been derived elsewhere.

Comparison with a Numerical Model

An axisymmetric, linear, triangular, finite-element model was developed using Matlab 5.2 to provide numerical solutions for comparison with the analytical solutions presented above. The model is used to provide greater confidence in, and a better understanding of, the analytic solutions.

The consistent formulation of Galerkin's method of weighted residuals is used for both s and $\partial s/\partial t$, using a linear variation with r and z (Segerlind 1984; Cheney and Kincaid 1994), while the trapezoid rule is used to integrate with respect to time. The generated mesh is finer near the pumping well boundary and becomes coarser with increasing radial distance. The mesh along the r-axis ranges from 0.03 to 1,000 m, while the z-axis ranges from 0 to 100 m. A mesh refinement program was used to increase the spatial density of nodes from an initial specification of 103 vertices and 169 triangles to a final geometry of 5,549 vertices and 10,816 triangles (Haborak 1999).

Boundary conditions were established for confined and leaky aquifers, as well as for a well that partially penetrates a confined aquifer. A pumping rate of 500 m^3/day, a frequency of three cycles/day (i.e., an 8-h period), a storativity of 1.6×10^{-6}, and a transmissivity of 51 m^2/day were specified for all simulations. The source well was fully screened between 35 and 60 m for the partially penetrating well problem. For the leaky case, the aquitard hydraulic conductivity was set at 0.03 m/day and the aquitard thickness was 10 m.

Two initial conditions were specified for each of the boundary value problems: (1) the initial drawdown is zero throughout the domain, and (2) the initial drawdown is equal to the analytical solution value at t=0 (simulating steady periodic conditions). The two initial conditions were used to evaluate the effect of the neglected initial transient terms in the analytical solution. The duration of the pumping period was set at 30 h using a time step of 3 min (600 time steps total). The solutions of the problems required a total of approximately 40 min on a 266-MHz Pentium II with 64 MB of RAM. The numerical and analytical predictions of drawdown were compared at t=6, 7.5, 10, 15, and 30 h.

Table 1 presents the root-mean squared differences between the numerical and analytical solutions within the modeled domain at nodes less than and greater than 2 m from the pumping well, expressed as the percentage of the analytical solution, for the case where the initial drawdown is zero. The division of nodes into two groups (i.e., less than and greater than 2 m from the pumped well) was made based on inspection of calculated errors—errors at nodes within 2 m were generally greater than errors at nodes outside of this zone.

The excellent agreement between numerical and analytical solutions, even within the 2-m zone, suggests that the analytical steady periodic solutions are consistent with the numerical model. Differences for the case where the initial condition were specified equal to the analytical solution are practically identical to those presented in Table 1, indicating that the effects of the initial transient can be neglected.

Nodes closer than 2 m show greater differences because of the assumption of an infinitesimal well diameter used to obtain the analytical solution. This assumption causes the analytical solution to approach infinity as the radial distance approaches zero; therefore, the analytical solutions do not accurately represent the physical system near the pumping well. Larger differences were found for the case where the initial condition was set equal to zero (e.g., 4.4% vs. 0.2% for the confined aquifer at distances greater than 2 m at 6 h), but these differences decreased by the end of the simulation period (e.g., 0.6% vs. 0.1% for the confined aquifer at distances greater than 2 m at 30 h), presumably due to the decay of the initial transient. It is also interesting to note that the differences for the confined aquifer at large distance are larger than for either the leaky or partially penetrating cases.

 DOI 10.1007/s10040-003-0255-7

Field Demonstration

Site Description

Sinusoidal aquifer tests were conducted at the Southwest Pad, shown in Fig. 1, which is located near the Burial Ground Complex at the Savannah River site. The Savannah River site is located in the Atlantic Coastal Plain physiographic province, which extends from Cape Cod, Massachusetts, to south-central Georgia. This province is underlain by seaward-dipping unconsolidated and poorly consolidated sediments that, in South Carolina, increase from a thickness of zero at the Fall Line (i.e., the uppermost extent of the Coastal Plain province) to more than 1,200 m at the coast. The sediments of the Atlantic Coastal Plain were deposited under a variety of conditions and have formed a complex system of transmissive and confining units. The Savannah River site is located near the updip edge of the Atlantic Coastal Plain sequence where the sedimentary wedge thins dramatically and undergoes abrupt facies changes (Aadland et al. 1995).

Table 2 presents the litho- and hydro-stratigraphy in the vicinity of the aquifer testing location. The Floridan Aquifer system is the uppermost system at the Savannah River site, and is the subject of investigation here. Tables 3 and 4 present representative values of selected hydrologic properties for aquifers and confining units, respectively, in the vicinity of the aquifer testing location (Aadland et al. 1995).

The Gordon Aquifer is the deepest aquifer within the Floridan Aquifer system and has a thickness that ranges from 20 to 30 m. The Green Clay Aquitard separates the Gordon Aquifer from the overlying Upper Three Runs Aquifer. The Green Clay, present at a depth between 30 and 50 m, includes abrupt facies changes from clay to silty and sandy material, with a thickness ranging from 0.6 to 3 m. The permeability of this unit varies greatly;

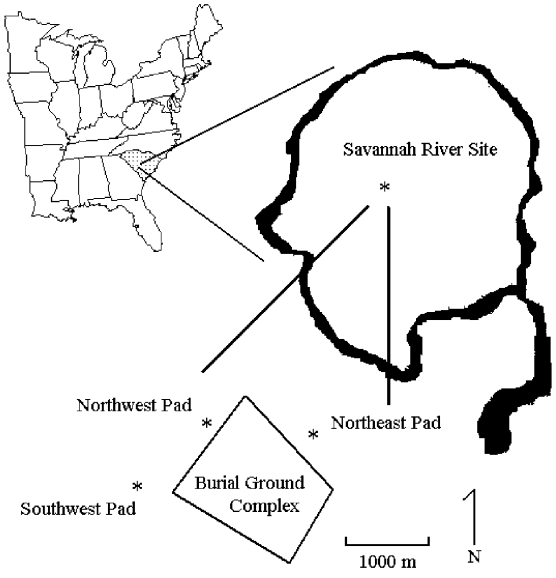

Fig. 1 General location map for the Southwest Pad, Burial Ground Complex, Savannah River site

Table 2 Representative litho- and hydro-stratigraphy of the Savannah River site

Lithostratigraphy			Hydrostratigraphy	
Age	Group	Formation	Unit	System
Miocene	Hawthorne	Altamaha (Upland)	Surficial Aquifer	Floridan Aquifer system
Eocene	Barnwell	Tobacco Road		
		Irwinton Sand[a]		
		Twiggs Clay[a]	Tan Clay Aquitard	
		Griffins Landing[a]	Barnwell-McBean Aquifer	
		Clinchfield		
	Orangeburg	Tinker/Santee		
		Warley Hill	Green Clay Aquitard	
		Congaree	Gordon Aquifer	
	Black Mingo	Fishburne/Fourmile		
Paleocene		Snapp/Williamsburg	Crouch Branch Aquitard	Meyers Branch Confining system
		Ellenton		
Cretaceous	Lumbee	Steel Creek/Peedee	Crouch Branch Aquifer	Dublin-Midville Aquifer system
		Black Creek		

[a] Members of Dry Branch Formation

Table 3 Representative hydrologic properties of aquifers, Burial Ground Complex, Savannah River site

Aquifer	Thickness (m)	Diffusivity, D (m^2/s)	Transmissivity, T (m^2/s)	Storativity, S
Surficial	3–12	0.07	0.8×10^{-3}	120×10^{-4}
Barnwell-McBean	12–40	4	0.6×10^{-3}	1.6×10^{-4}
Gordon	20–30	10	2.5×10^{-3}	2.5×10^{-4}
Crouch Branch	75	78	31×10^{-3}	4.0×10^{-4}

 DOI 10.1007/s10040-003-0255-7

Table 4 Representative hydrologic properties of confining units, Burial Ground Complex

Confining unit	Thickness, m′ (m)	Vertical hydraulic conductivity, K' (m/s)	Leakance, $L=K'/m'$ (L/s)
Tan Clay	1.5–8	2.11×10^{-9}	3.0×10^{-10}
Green Clay	0.6–3	0.64×10^{-9}	3.2×10^{-10}
Crouch Branch	18	1.10×10^{-9}	0.58×10^{-10}

zones within this unit can be locally confining, semi-confining (leaky), or transmissive.

The Upper Three Runs Aquifer lies above the Green Clay Aquitard, and is subdivided into an Upper Unit and a Lower Unit. The Lower Unit is commonly referred to as the Barnwell-McBean Aquifer, and is a poorly defined, semi-confined aquifer ranging in thickness from 12 to 40 m. This aquifer consists mainly of sands and fine-grained material, but limestone can be found in the lower section of the unit. The Tan Clay Aquitard separates the Upper and Lower Units. The Tan Clay is a semi-confining (leaky) layer formed by lenses of clay and sandy clay, ranging in thickness from 0 to 8 m. The Upper Unit (also called the Surficial Aquifer) is an unconfined aquifer that lies above the Tan Clay, and is encountered at depths down to 25 m below ground surface, and varies in saturated thickness from 3 to 12 m.

Precipitation recharges the Surficial Aquifer, and discharge occurs by leakage into underlying aquifers as well as by seepage into local perennial streams to the north and south. Flow into and through underlying aquifers also migrates to regional discharge points in more distant rivers and streams.

All three aquifers within the Floridan Aquifer System were examined in this study. The test facility contains one pumping well within each aquifer of the three aquifers, along with two observation wells in the Surficial Aquifer and the Barnwell-McBean Aquifer, and three observation wells in the Gordon Aquifers. Figure 2 presents plan and profile views of the Southwest Pad configuration.

Equipment

The field testing equipment was designed to honor several objectives, including: (1) the incorporation of off-the-shelf components, (2) the need for portability and ease of field setup, and (3) the need to constrain costs. Because technology transfer from this research project to the general public was an important consideration, it was believed that honoring the above objectives would facilitate use by others.

Figure 3 is a schematic of the field setup. The control and monitoring system was designed around the CR23X datalogger (Campbell Scientific, Inc., Logan, UT). The datalogger is equipped with digital input–output control ports, and differential analog- and constant-voltage channels for controlling and monitoring pressure transducers, solenoid valves, flow meters, and pumping rates. The datalogger has an RS-232 port that allows continuous monitoring with a portable computer. The datalogger was programmed to minimize power usage during operations so that a single, deep-cycle marine battery provided ample power for the datalogger operation.

Sinusoidal pumping rates were controlled using a Variable Frequency Drive (VFD, Model Redi-Flo, Grundfos Pumps Corp., Clovis, CA), which provides 120 VAC power for the pumps. The frequency response (ω) of the VFD was controlled by a 4- to 20-mA signal converted from voltage output of the datalogger (±5 V) using a signal control module (model SCM5B39–2, Dataforth, Tucson, AZ). The range of frequencies available to the pumps ranged from 0 to 100 Hz. Sensitivity of the pumping control system (i.e., $d\omega/dV$) was determined to be 10.2±0.005 Hz/V.

Two Grundfos, 10-cm (4-inch) Redi-Flow Variable Performance Pumps (model 16E4, Grundfos Pumps Corp., Clovis, CA) were used in the field. The first pump was used for withdrawing water from the target well, and the second pump was used for reinjection. The reinjection pump was installed horizontally in a portable, 79-m^3 container (Rain for Rent, Charlotte, NC) and secured with concrete blocks. At least 20 cm of water was maintained above the pump intake to prevent cavitation. The 16E4 pumps are capable of flows that range from 0.1 to 92.6 L/min, depending on the dynamic head losses and the frequency settings on the VFD.

Flow rates in each direction were monitored with separate flow meters (model FP5300, Omega Engineering, Stamford, CT) connected to the datalogger through magnetic amplifiers (model FLSC-AMP-A, Omega Engineering) that filter high-frequency noise and boost signal output. Withdrawal and injection flow lines were opened and closed using normally closed, zero-differential solenoid valves (model S20, GC Valves, Simi Valley, CA). The valves fully seal when de-energized without the need for backpressure, a requirement in this field setup where backpressure on both the pumping and injection directions would range from 0 to 3 m maximum.

Powering the system required the use of several relays, all controlled by the datalogger. A double-throw latching relay (model HD4850, Crydom, San Diego, CA) was energized by the datalogger to turn the VFD on and off, which was needed before switching flow directions. The second set of relays (all model D2425, Crydom) split the AC power cable from the VFD to the pumps. Because the pumps required three-phase power, three relays were needed for each pump, which were energized by a fourth relay (model D1D07, Crydom) controlled by the datalogger. The relays, mounted on a single board, made the purchasing of a second VFD unnecessary, reducing equipment costs by several thousand dollars. A third set of relays (model D1D07) energized the two solenoid

 DOI 10.1007/s10040-003-0255-7

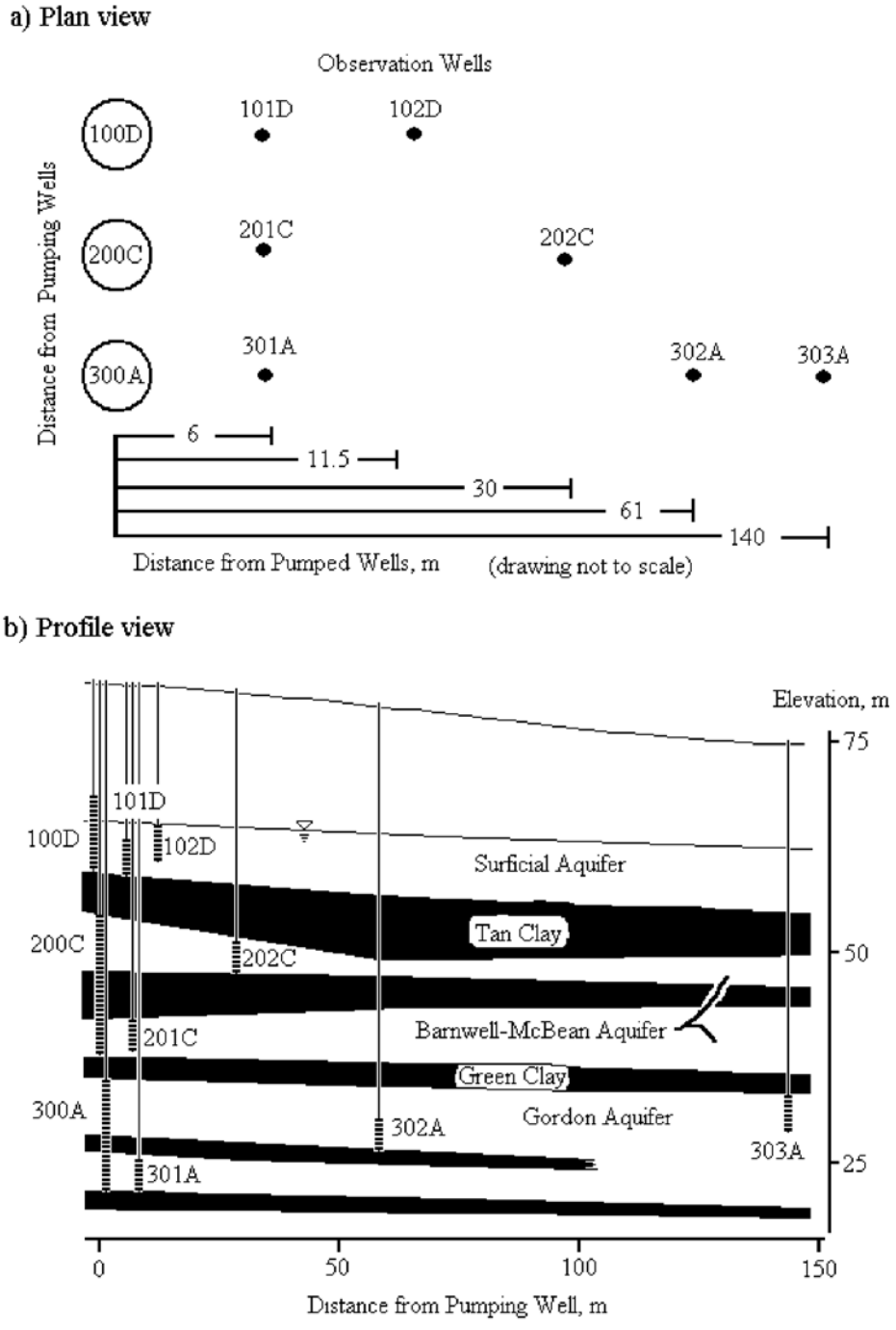

Fig. 2 Site configuration for the Southwest Pad: **a** plan view, **b** profile view

valves. All relays were DC powered by a single, deep-cycle marine battery. A 30-amp portable generator supplied AC power to the pumps.

Pressure transducers (model PDCR 1830-8388, Druck, Inc., New Fairfield, CT) were installed inside the pumping well and portable water container to monitor change in water levels, and for calculations of head loss during the aquifer tests. Additional gauge pressure transducers (model PDCR 830-0576, Druck, Inc., New Fairfield, CT) were tied to multiple CR-10 dataloggers (Campbell Scientific, Inc., Logan, UT) installed at all monitoring wells. In addition to monitoring water levels in each of the pumping wells (SWP 100D, SWP 200C, and SWP 300A), two observation wells (SWP 101D and SWP 102D) were used to monitor water levels in the Surficial Aquifer, two in the Barnwell-McBean Aquifer (SWP 201C and SWP 202C), and three in the Gordon Aquifer (SWP 301A, SWP 302A, and SWP 303A).

 DOI 10.1007/s10040-003-0255-7

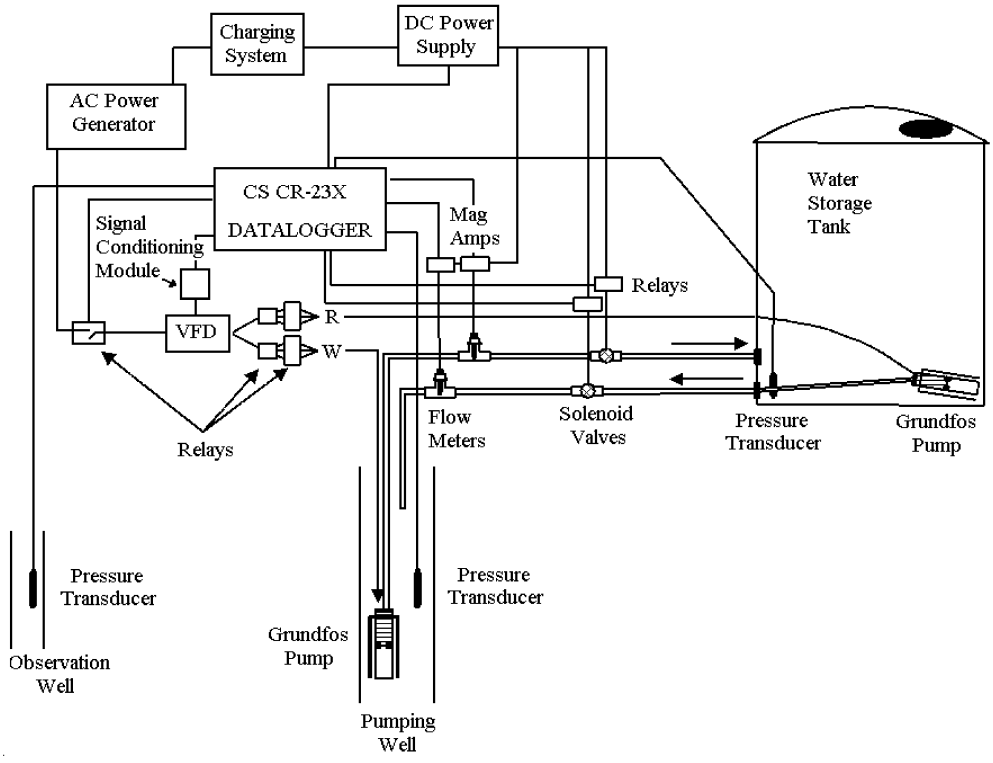

Fig. 3 Field configuration and wiring diagram for sinusoidal aquifer test

Table 5 Sinusoidal aquifer test conditions, Southwest Pad

Aquifer	Pumped well	Period, p (h)	Cycles (n)	Pumping rate amplitude, $\|Q\|$ (L/s)
Surficial	SWP 100D	1	4	0.416
Barnwell-McBean	SWP 200C	2	4	1.190
Gordon	SWP 300A	2.5	3	1.079

Aquifer Test Interpretation

Aquifer Test Conditions

Table 5 presents the aquifer test conditions for the sinusoidal aquifer tests in each of the three aquifers evaluated. Note that multiple cycles were used to obtain repetitions of each complete cycle. The first step in aquifer test interpretation is to fit the pumping well flow rate using ordinary least squares. This is done by establishing the sinusoidal function as:

26-30
5 notes:

$$= os\ \omega t + \quad in\ \omega \quad (26)$$

where $\omega=2\pi/p$ is the specified frequency of the induced pumping, p is the pumping cycle period, and t is the time from the beginning of the aquifer test. In this case, the pumping rate, $Q(t)$ and the cosine and sine terms are known, and the objective is to estimate the unknown coefficients, Q_1 and Q_2. The amplitude, Q_o, and phase lag, φ_Q, of the pumping rate are then calculated using:

$$Q_o = |Q| = \sqrt{Q_1^2 + Q_2^2} \quad (27)$$

$$\phi_Q = atan\frac{Q_2}{Q_1} \quad (28)$$

Aquifer drawdowns in observation wells are also fit using sinusoidal functions in the same manner.

$$s(t) = s_1\ cos\,\omega t + s_2\ sin\,\omega t \quad (29)$$

To simplify interpretation, the amplitude and phase lag of observation-well drawdowns were further adjusted to yield unit drawdowns that corresponds to the drawdown amplitude and phase lag corresponding to a unit (cosine) pumping rate:

$$s_o = \frac{|s|}{|Q|} = \frac{\sqrt{s_1^2 + s_2^2}}{\sqrt{Q_1^2 + Q_2^2}} \quad (30)$$

$$\phi_o = \phi_s - \phi_Q = atan\frac{s_2}{s_1} - atan\frac{Q_2}{Q_1} \quad (31)$$

where s_o is the drawdown amplitude per unit pumping amplitude and φ_o is phase lag between the observed drawdown and the imposed pumping. If needed, the phase lag can also be expressed in units of radians by dividing the phase lag expressed in units of time by the pumping frequency, i.e., $\phi\ (rad)=\phi\ (time)/\omega$.

Figure 4 presents the observed pumping rates, Q, and drawdowns, s, along with best-fit sinusoidal functions. Table 6 summarizes pumping data and water level

 DOI 10.1007/s10040-003-0255-7

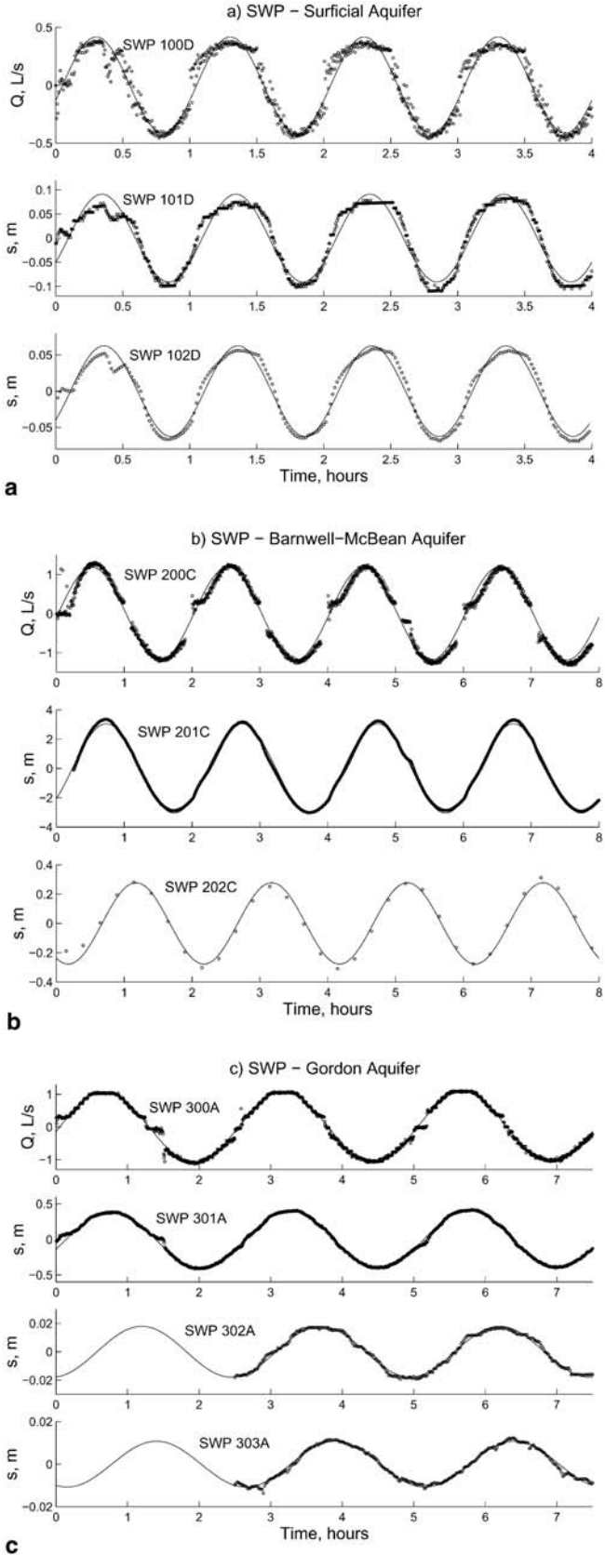

Fig. 4 Observed and fitted pumping rate, Q, and drawdowns, s, for **a** the Surficial Aquifer, **b** Barnwell-McBean Aquifer, and **c** Gordon Aquifer at the Southwest Pad

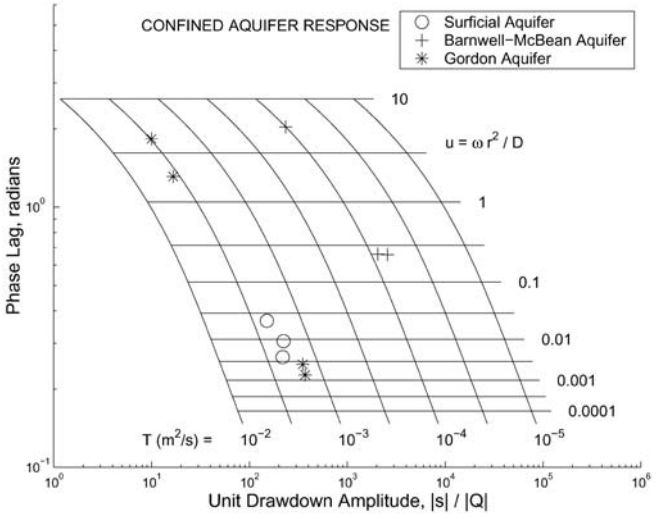

Fig. 5 Response surface contours of transmissivity, T, and well argument, u, for confined aquifers as a function of unit drawdown amplitude and phase lag. Plotting positions of individual well responses also shown

responses to pumping. Multiple responses are shown in several wells (SWP 100D, SWP 101D, SWP 201C, and SWP 301A) because multiple pressure transducers and dataloggers provided redundant measurements in these cases.

Note that the positive limbs in Fig. 4 are shaped differently from the negative limbs. This results from the need to employ two separate pumping systems: one to lift water from the borehole into the storage container, and a second system to return water from the storage container back to the borehole. Also note that the shape of the pumping rate is least symmetric for the first aquifer tested (the Surficial Aquifer), but improves for later tests (the Gordon Aquifer). This improvement results from adaptive improvements in the datalogger pumping control logic during the progress of the tests.

Confined Aquifer Response

One way to interpret observed phase lags and amplitudes is to form a parameter surface for these two variables. Figure 5 presents the parametric surface for aquifer transmissivity, T, and dimensionless confined aquifer argument, $u=\omega\ r^2/D$, for a range of unit drawdown amplitudes, $s_o=|s|/|Q|$, and phase lags, $\phi_o=\phi_s-\phi_Q$. Also shown in Fig. 5 are the plotting positions of individual well responses.

Note that changes in the unit drawdown amplitude directly affect the transmissivity, but do not affect the well function argument. Instead, the well function argument is directly affected by the phase lag. While order-of-magnitude estimates can be obtained using Fig. 5, the relationship between u and φ_o can be used to obtain more precise estimates. The method first uses the observed phase lag to estimate the value of u, and then u is used to estimate the aquifer hydraulic diffusivity.

 DOI 10.1007/s10040-003-0255-7

Table 6 Observed water level responses to sinusoidal pumping. Well ID: *D* Surficial Aquifer; *C* Barnwell-McBean Aquifer; *A* Gordon Aquifer

Well ID	Well radius (cm)	Well distance (m)	Screen zone		Datalogger	Unit drawdown amplitude[a] (s/m^2)	Phase lag (min)
			Elevation (m, a.m.s.l.)	Length (m)			
SWP 100D	7.6	0.0	63.5	9.1	CR-23	7,828	1.77
					CR-10	7,485	1.79
SWP 101D	2.5	6.1	60.7	3.0	CR-23	219	2.53
					CR-10	223	2.92
SWP 102D	2.5	11.5	62.5	3.0	CR-10	151	3.49
SWP 200C	7.6	0.0	45.9	18.3	CR-23	6,613	3.72
SWP 201C	2.5	6.3	39.0	3.0	CR-23	2,568	10.81
					CR-10	2,055	10.86
SWP 202C	2.5	30.1	48.7	3.0	CR-10	234	37.05
SWP 300A	5.1	0.0	26.4	12.2	CR-23	4,169	4.53
SWP 301A	2.5	5.5	23.0	3.0	CR-23	371	5.41
					CR-10	350	5.93
SWP 302A	2.5	60.6	27.6	3.0	CR-10	17	31.33
SWP 303A	2.5	139.8	30.4	3.0	CR-10	10	43.66

[a] Unit drawdown amplitude is the amplitude of the water level change divided by the amplitude of the pumping rate, $|s|/|Q|$

Table 7 Summary of parameter estimates for sinusoidal aquifer tests. Well ID: *D* Surficial Aquifer; *C* Barnwell-McBean Aquifer; *A* Gordon Aquifer

Well ID	Datalogger	u	D (m^2/s)	T (m^2/s)	S
SWP 101D	CR-23	4.01×10^{-3}	16.07	21.7×10^{-4}	1.35×10^{-4}
	CR-10	9.13×10^{-3}	7.09	18.5×10^{-4}	2.61×10^{-4}
SWP 102D	CR-10	23.10×10^{-3}	9.96	22.7×10^{-4}	2.28×10^{-4}
SWP 201C	CR-23	0.239	0.15	0.69×10^{-4}	4.74×10^{-4}
	CR-10	0.242	0.14	0.85×10^{-4}	5.97×10^{-4}
SWP 202C	CR-10	5.52	0.14	1.02×10^{-4}	7.10×10^{-4}
SWP 301A	CR-23	1.41×10^{-3}	14.85	15.0×10^{-4}	1.01×10^{-4}
	CR-10	2.64×10^{-3}	8.03	14.7×10^{-4}	1.83×10^{-4}
SWP 302A	CR-10	1.86	1.38	37.0×10^{-4}	26.8×10^{-4}
SWP 303A	CR-10	4.29	3.56	30.8×10^{-4}	8.64×10^{-4}

The aquifer hydraulic diffusivity for a confined aquifer is estimated using Eq. (8), which specifies the relationship between the phase lag, ϕ_o, the pumping frequency, ω, the distance from the pumping well, r, and the hydraulic diffusivity, D. This relationship can be written as:

$$\phi_o = \mathrm{F}(u) = arg\left\{K_o\left(\sqrt{\mathbf{i}u}\right)\right\} \tag{32}$$

where u is the principal unknown. Given that the phase lag has already been calculated using Eq. (31), this equation can be solved for u by inversion to obtain a unique estimate of the well function, $u=\mathrm{F}^{-1}(\phi_o)$, in which the inverse function is approximated using a fifth-order, logarithmic polynomial:

$$ln\ u = \int_{i=o}^{5} c_i\,(ln\,\phi_o)^i \tag{33}$$

where c=[–0.12665, 2.8642, –0.47779, 0.16586, –0.076402, 0.03089].

Thus, the first step is to use the estimated phase lag in Eq. (31) to obtain u. The aquifer diffusivity, D, is then readily found using:

$$D = \frac{\omega\, r^2}{u} \tag{34}$$

The aquifer transmissivity, T, is then determined by rearranging Eq. (7):

$$T = \frac{|Q|\left|K_o(\sqrt{\mathbf{i}u})\right|}{2\pi|s|} = \frac{\left|K_o(\sqrt{\mathbf{i}u})\right|}{2\pi s_o} \tag{35}$$

Finally, the aquifer storativity is found using $S=T/D$.

Tables 7 and 8 summarize the estimated aquifer parameters, arranged by aquifer. It is interesting to note the small values of the aquifer storativity for the Surficial Aquifer. In effect, the aquifer test period is too short to induce delayed yield, and appears to only induce elastic storage of water. All aquifers were treated as confined, even the Surficial Aquifer. The use of a confined model for the Surficial Aquifer is justified in this analysis for two reasons: (1) the amplitude of the disturbance in the Surficial Aquifer is small (less than 3% of the thickness of the aquifer), and (2) the calculated aquifer storativity is very small, less than 3×10^{-4}, which is consistent with confined behavior.

 DOI 10.1007/s10040-003-0255-7

Table 8 Summary of parameter estimates for constant-discharge aquifer tests. Well ID: *D* Surficial Aquifer; *C* Barnwell-McBean Aquifer; *A* Gordon Aquifer

Well ID	*D* (m^2/s)	*T* (m^2/s)	*S*
SWP 101D	40.83	9.80×10^{-4}	0.24
SWP 102D	31.38	8.16×10^{-4}	0.26
SWP 201C	0.09	0.78×10^{-4}	8.77×10^{-4}
SWP 202C	0.27	1.29×10^{-4}	4.86×10^{-4}
SWP 301A	0.67	5.18×10^{-4}	7.72×10^{-4}
SWP 302A	1.36	25.35×10^{-4}	18.7×10^{-4}
SWP 303A	3.72	24.46×10^{-4}	6.57×10^{-4}

Leaky Aquifer Response

The effect of leakage on aquifer parameters was evaluated qualitatively by comparing observed drawdown amplitudes and phase lags with leaky aquifer response curves. Response curves are constructed so that all aquifer tests can be compared on a single plot. Leaky aquifer response curves can be constructed for a range of well arguments, u, and leakage, $v=(r/B)^2$, using Eq. (15):

$$s_e = \left|K_o(\sqrt{\mathbf{i}u + v})\right| \tag{36}$$

where $s_e=2\pi\ T\ |s|/|Q|$ is the dimensionless drawdown amplitude. The confined aquifer model can be used to provide an initial estimate of the aquifer transmissivity, i.e., Eq. (35).

Plots of dimensionless drawdown amplitude and phase lags are shown in Fig. 6, along with response curves for representative values of v=0.1, 0.01, and 0.0001. Inspection of the figure indicates that increasing the leakage parameter causes the response curve to shift to the left (i.e., lower dimensionless drawdown amplitudes) for smaller phase lags. The effects of leakage should manifest themselves by displaying a smaller dimensionless drawdown amplitude when the phase lag is small.

Observed aquifer responses for sinusoidal tests conducted at the Southwest Pad tend to fall along the confined aquifer type curve (v=0), and none of the leaky aquifer type curves appear to match observed amplitudes. Leakage between units cannot be estimated from the data, and longer period cycles are required if estimates of aquifer leakage are needed.

While the most distant points (i.e., the observation wells with the smallest amplitudes and largest phase lags) fall below the confined aquifer curve, this is more likely due to spatial heterogeneity within the aquifer than due to the effects of leakage. As shown in the profile view in Fig. 2, well screens in observation wells located away from the pumped well (Wells SWP 302A and 303A) are positioned above a clay lens, while the well screen in the nearest well (Well SWP 301A) lies below the clay lens.

Partially Penetrating Aquifer Response

The observation wells at the Southwest Pad only partially penetrate the aquifer. Parameter estimate should not be affected when the pumping well fully penetrates a confined aquifer with no leakage. In other situations, however, the pumping well screen may not fully span the aquifer, and the hydraulic response at observation wells may be affected.

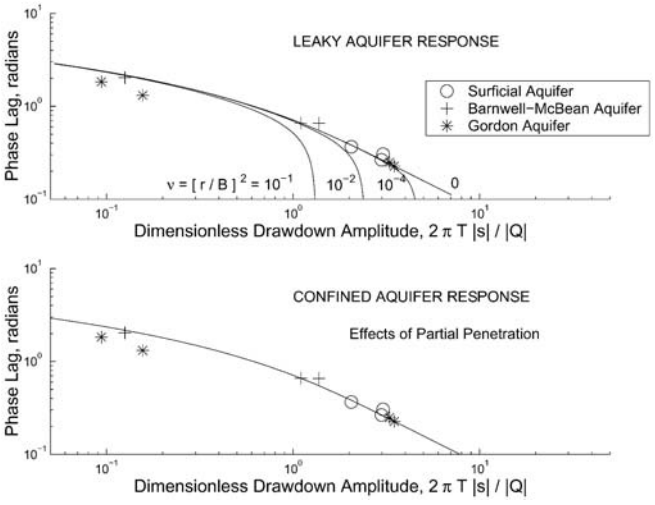

Fig. 6 Response curves for leaky aquifers (*above*) and the predicted effects of partial penetration at the Southwest Pad (*below*)

The magnitude of the effects of a partially penetrating pumping and/or observation well depends on the configuration of the pumping and observation well screens. As a result, a response curve that applies to all configurations is substantially more difficult to construct. Instead, known screen lengths and positions can be used to generate response curves for the specific problem of concern using Eq. (23).

As an exercise, the effects of partial penetration were evaluated at the Southwest Pad. Observation well screened intervals are all 3 m in length. The screened zone in the pumping wells is 9.1 m for the Surficial Aquifer (Well SWP 100D), 18.3 m for the Barnwell-McBean Aquifer (Well SWP 200C), and 12.2 m for the Gordon Aquifer (Well SWP-300A).

Figure 6 shows the confined aquifer response curve along with partial penetration response curves corresponding to aquifer conditions at the Southwest Pad. Note that in all cases the response curves corresponding to partial penetration overlay the confined aquifer curve. Clearly, the effects of partial penetration are not important for the field conditions at the Southwest Pad when a sinusoidal pumping rate is used.

If the effects of partial penetration are a concern, then a response curve can be constructed for known aquifer and well-screen geometries. The computed response curve should then be used instead of Eq. (32). The aquifer hydraulic diffusivity can be estimated using a new form of Eq. (33) for the problem of interest, and the transmissivity estimated using the form analogous to Eq. (35). The aquifer storativity is again estimated using $S=T/D$.

 DOI 10.1007/s10040-003-0255-7

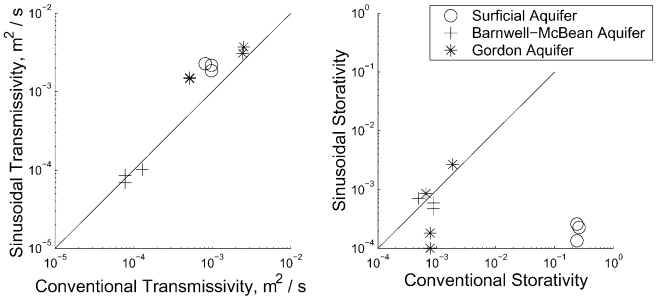

Fig. 7 Comparison of conventional vs. sinusoidal aquifer hydraulic parameters: transmissivity (*left*) and storativity (*right*). Lines of equality also shown

Comparison of Results

Table 7 presents unpublished aquifer testing results from the Southwest Pad (Westinghouse Savannah River Corporation 1999). The aquifer parameters were estimated using conventional aquifer tests with an aquifer test duration of 72 h and pumping rates of 0.48, 1.38, and 2.71 L/s for SWP 100D, SWP 200C, and SWP 300A, respectively. Interpreted aquifer test results were not provided by the Savannah River site until after estimates of aquifer parameters had been obtained, and were not used for assistance in estimating aquifer parameters. Figure 7 presents a comparison of conventionally estimated aquifer hydraulic properties with the sinusoidal estimates collected in this study.

Note that sinusoidally estimated transmissivities are within an order-of-magnitude of the conventional estimates. There is a monotonic increase in both, from smallest to largest, although the sinusoidal estimates are larger than the conventional estimates. No explanation for the observed differences is apparent.

The storativity properties are markedly different between the two approaches, however. Most striking is the discrepancy within the Surficial Aquifer. The conventional tests resulted in an estimated specific yield of 0.24 to 0.26, while the sinusoidal test yielded an estimate of storativity of 1.35 to 2.61×10^{-4}. It appears that the sinusoidal test never causes a lowering of the water table; instead, a release from storage due to an elastic response is observed.

Also, the storativity at the nearer well within the Gordon Aquifer is substantially different, 7.72×10^{-4} vs. $1.01–1.83\times10^{-4}$. This difference may result, in part, from the effects of borehole storage. The advantage of the pumping control equipment used during the sinusoidal tests allows the specification of the flux at the borehole wall, rather than from the pump itself (Young et al. 2002). The effects of dynamic head losses and borehole storage can be monitored and the pumping rate can be adjusted to deliver a specified flux at the borehole wall. Thus, improved pumping rates are obtained by monitoring borehole storage from water-level changes within the borehole, and by using flowmeters to account for dynamic head losses.

Summary

A procedure for conducting and interpreting sinusoidal aquifer tests is presented for confined, leaky, and partially penetrating aquifers. The analytical solution for sinusoidal pumping in a confined aquifer system is identical to that presented by Bruggeman (1999) but different from a solution presented by Black and Kipp (1981) which only involves the aquifer hydraulic diffusivity, and not the aquifer transmissivity or storativity. The analytical solution for a leaky aquifer corrects a solution presented by Bruggeman (1999). A new analytical solution is presented for a well that partially penetrates a confined aquifer.

The analytical solutions were compared with a finite element simulation model. Excellent agreement between the analytical and numerical solutions was found except in the region less than 2 m from the pumping well. The discrepancy is consistent with the borehole-wall boundary condition in the analytical solution, which assumes an infinitesimal borehole diameter.

The proposed procedure was demonstrated at the Savannah River site, Burial Ground Complex, where sinusoidal tests were conducted in a surficial aquifer and two confined sedimentary aquifers typical of the Atlantic Coastal Plain. The field testing system employed a datalogger, a variable-speed pump to lift water from the borehole into a mobile container, a second pump to reinject water from the container into the borehole, paddle-wheel flow meters to monitor pumping rates, and pressure transducers to monitor water levels in the pumping and observation wells. All pumped fluids were returned to the formation from which they were pumped, and no investigation-derived wastes were generated.

Aquifer hydraulic properties estimated using this procedure for the deeper aquifers are consistent with previous studies. The match between estimates is inconsistent for the surficial aquifer because the conventional aquifer tests yielded estimates of the specific yield (consistent with an unconfined response), while the shorter-duration sinusoidal perturbations yielded estimates of the storativity (consistent with a confined, elastic response).

The utility of the approach lies in its ability to eliminate, or substantially minimize, investigation-derived wastes, which may be of significant concern at locations where contaminated fluids must be disposed of in an environmentally acceptable manner. An additional advantage is the ability to introduce a signal that is substantially different from background perturbations, thus easing detection of the signal at observation wells.

Many questions associated with the use of this technique remain, however. Analytic solutions for other conditions (e.g., dual porosity aquifers, unconfined aquifers, storage in the confining layer) have yet to be developed for sinusoidal pumping. Also, interpretation methods for data obtained from single-well tests are needed. Finally, guidance on the selection of the appropriate pumping frequency, as well as the utility of

 DOI 10.1007/s10040-003-0255-7

31-33
3 notes:

pumping at multiple frequencies, would assist in optimizing the efficiency of the technique.

Acknowledgments This research was funded by a grant from the US Department of Energy (DOE004) through the Education, Research and Development Association of Georgia Universities (ERDA). We wish to express appreciation to Ratib Karam of ERDA for overall project support, Mark Amidon of Westinghouse Savannah River Company for providing access to the Southwest Pad, Paul Wentston at the University of Georgia for his finite-element, mesh-refinement code, and Kurt Pennell of the Georgia Institute of Technology for access to laboratory facilities. We are greatly indebted to Diana Allen, Bill Lanyon, Perry Olcott, John Barker, and several anonymous reviewers for their helpful comments.

34
Tanmoy Das

Appendix

This appendix presents derivations for the hydraulic response to sinusoidal pumping in three types of aquifers: fully penetrating wells in confined aquifers, fully penetrating wells in leaky aquifers, and partially penetrating wells in confined aquifers.

35
Tanmoy Das

The approach follows the conventional method of obtaining solutions for constant pumping problems, except that the pumping rate is now treated as a complex coefficient.

The solutions are obtained by first using the Laplace transform to eliminate the time derivative, and then, for the partially penetrating problem, by using the finite Fourier cosine transform to eliminate the derivative with respect to the vertical dimension. Analytical solutions in the transformed domain are then inverse-transformed to provide aquifer responses in time. Alternatively, the inverse-transforms could be performed numerically, if desired.

36
Tanmoy Das

Derivation of Confined Aquifer Response

The response of a confined aquifer to sinusoidal pumping is obtained by the use of Laplace transforms. The Laplace transform of an arbitrary function $f(r,t)$ with respect to t and p is defined as:

$$L\{f(r,t)\} = \bar{f}(r,p) = \int_o^\infty e^{-pt} f(r,t)\, dt \tag{37}$$

and has the property that:

$$L\{f'(r,t)\} = p\bar{f}(r,p) - f(r,0) \tag{38}$$

where the prime denotes differentiation with respect to time (Carslaw and Jaeger 1953; Poularikas 1996). Taking the Laplace transform with respect to t and p of Eq. (2), (4), and (5) using Eq. (37) and (38) yields:

$$\frac{\partial^2 \bar{s}}{\partial r^2} + \frac{1}{r}\frac{\partial \bar{s}}{\partial r} - \frac{p}{D}\bar{s} = 0 \tag{39}$$

$$\bar{s}\,(\infty, p) = 0 \tag{40}$$

$$\lim_{r\to 0}\; r\,\frac{\partial \bar{s}}{\partial r} = \frac{-Q_o}{2\pi T}\frac{1}{p - \mathbf{i}\omega} \tag{41}$$

Equation (39) is the modified Bessel differential equation of zero order and has the general solution

$$\bar{s}(r,p) = A_1\, K_o\left(r\sqrt{\frac{p}{D}}\right) + A_2\, I_o\left(r\sqrt{\frac{p}{D}}\right) \tag{42}$$

where I_o and K_o are the zero-order modified Bessel functions of the first and second kind, respectively, and A_1 and A_2 are constants. Equation (40) can be used to show that A_2=0, because $I_o \to \infty$ as $r \to \infty$.

It can be shown that:

$$\lim_{u\to 0}\; u\,\frac{dK_o(u)}{du} = 1 \tag{43}$$

because:

$$\frac{dK_o(x)}{dx} = K_1(x) \tag{44}$$

and:

$$\lim_{x\to 0}\; x\,K_1(x) = 1 \tag{45}$$

so that:

$$A_1 = \frac{Q_o}{2\pi T(p - \mathbf{i}\omega)} \tag{46}$$

resulting in:

$$\bar{s}(r,p) = \frac{Q_o}{2\pi T(p - \mathbf{i}\omega)} K_o\left(r\sqrt{\frac{p}{D}}\right) \tag{47}$$

Convolution can be used to obtain the inverse Laplace transform of Eq. (47) (Haborak 1999), yielding:

$$s(r,t) = \frac{Q}{2\pi T}\left[K_o\left(r\sqrt{\frac{\mathbf{i}\omega}{D}}\right) - \int_o^\infty \frac{\lambda\, J_o(r\lambda)}{\frac{\mathbf{i}\omega}{D} + \lambda^2}\; e^{-(\mathbf{i}\omega + D\lambda^2)t} d\lambda\right] \tag{48}$$

The first term within the brackets is the steady periodic response, while the second term is an initial transient response. If the second term is important, then a brief period may be necessary to allow the initial transient to dissipate. The initial transient results from quiescent conditions at the beginning of the test, in which the initial water levels are assumed to be static, rather than at steady periodic conditions.

Derivation of Leaky Aquifer Response

The response of a confined aquifer to sinusoidal pumping is obtained by taking the Laplace transform of the governing equation, yielding:

$$\frac{\partial^2 \bar{s}}{\partial r^2} + \frac{1}{r}\frac{\partial \bar{s}}{\partial r} - \left(\frac{1}{B^2} + \frac{p}{D}\right)\bar{s} = 0 \tag{49}$$

$$\bar{s}(\infty, p) = 0 \tag{50}$$

 DOI 10.1007/s10040-003-0255-7

$$\lim_{r\to 0}\ r\ \frac{\partial \bar{s}}{\partial r} = \frac{-Q_o}{2\,\pi\ T}\ \frac{1}{p-\mathbf{i}\omega} \tag{51}$$

Equation (49) is the modified Bessel differential equation of zero order and has the general solution:

$$\bar{s}(r,p) = A_1\ K_o\left(r\ \sqrt{\frac{p}{D}+\frac{1}{B^2}}\right)\ +\ A_2\ I_o\left(r\ \sqrt{\frac{p}{D}+\frac{1}{B^2}}\right) \tag{52}$$

which reduces to:

$$s_l(r,p) = \frac{-Q_o}{2\,\pi\ T(p-\mathbf{i}\omega)}\ K_o\left(r\ \sqrt{\frac{p}{D}+\frac{1}{B^2}}\right) \tag{53}$$

because A_2=0. Convolution can be used to obtain the inverse Laplace transform (Haborak 1999), resulting in:

$$s(r,t) = \frac{Q}{2\pi T}\left[K_o\left(r\ \sqrt{\frac{\mathbf{i}\omega}{D}+\frac{1}{B^2}}\right) - \int_o^{\infty}\frac{\lambda\, J_o(r\lambda)}{\frac{\mathbf{i}\omega}{D}+\frac{1}{B^2}+\lambda^2}e^{-(\mathbf{i}\omega+\frac{D}{B^2}+D\lambda^2)\ t}d\lambda\right] \tag{54}$$

The first term inside the brackets is again the steady periodic response, while the second term is the transient response to initial conditions.

Response in Partially Penetrating Wells

The derivation of the solution to the partially penetrating boundary value problem is found by first obtaining the Laplace transform with respect to t of Eqs. (17) and (19), (20), (21), and (22):

$$\frac{\partial^2 \bar{s}}{\partial r^2}+\frac{1}{r}\frac{\partial \bar{s}}{\partial r}+\frac{\partial^2 \bar{s}}{\partial z^2}-\frac{p}{D}\bar{s} = 0 \tag{55}$$

$$\bar{s}(\infty,z,p) = 0 \tag{56}$$

$$\left.\frac{\partial \bar{s}}{\partial z}\right|_{z=0} = 0 \tag{57}$$

$$\left.\frac{\partial \bar{s}}{\partial z}\right|_{z=m} = 0 \tag{58}$$

$$\lim_{r\to 0}\ r\ \frac{\partial \bar{s}}{\partial r} = \begin{cases} 0 & 0\le z<d \\ \frac{-Q_o}{2\pi\ K(l-d)\ (p-\mathbf{i}\omega)} & d\le z\le l \\ 0 & l<z\le m \end{cases} \tag{59}$$

Given a function defined in the interval $0\le z\le m$, the finite Fourier cosine transform with respect to z and m is defined as:

$$F_c\{f(r,z,t)\} = f_c(r,n,t) = \int_o^m f(r,z,t)\ cos\frac{n\pi z}{m}\ dz \tag{60}$$

where n=0, 1, 2,.... The transform has the property that:

$$F_c\{f''(r,z,t)\} = -\left(\frac{n\pi}{b}\right)^2 f_c(r,n,t)+(-1)^n f'(r,m,t) - f'(r,0,t) \tag{61}$$

where the prime denotes differentiation with respect to z (Miles 1971; Pinkus and Zafrany 1977; Sneddon 1972).

Taking the finite Fourier cosine transform from 0 to m of Eq. (55) with respect to z and n yields:

$$\frac{\partial^2 \bar{s}_c}{\partial r^2}+\frac{1}{r}\frac{\partial \bar{s}_c}{\partial r}-\frac{p\bar{s}_c}{D}-\left[\frac{n\pi}{m}\right]^2\bar{s}_c+(-1)^n f'(r,m,p) - f'(r,0,p) = 0 \tag{62}$$

which, upon substitution of Eqs. (57) and (58), yields:

$$\frac{\partial^2 \bar{s}_c}{\partial r^2}+\frac{1}{r}\frac{\partial \bar{s}_c}{\partial r}-\left[\frac{p}{D}+\left(\frac{n\pi}{m}\right)^2\right]\bar{s}_c = 0 \tag{63}$$

Equation (63) is the modified Bessel differential equation of zero order and has the general solution:

$$\bar{s}_c(r,n,p) = A_{1,n}K_o\left[r\ \sqrt{\frac{p}{D}+\left(\frac{n\pi}{m}\right)^2}\right] + A_{2,n}I_o\left[r\ \sqrt{\frac{p}{D}+\left(\frac{n\pi}{m}\right)^2}\right] \tag{64}$$

Equations (56) and (59) become:

$$\bar{s}_c(\infty,n,p) = 0 \tag{65}$$

$$\lim_{r\to 0}\ r\ \frac{\partial \bar{s}_c}{\partial r} = \int_d^l \frac{-Q_o}{2\pi K(l-d)(p-\mathbf{i}\omega)}cos\frac{n\pi z}{m}dz \tag{66}$$

The integral of this function for n=0 is:

$$\lim_{r\to 0}\ r\ \frac{\partial \bar{s}_c}{\partial r} = \frac{-Q_o}{2\,\pi\ K(p-\mathbf{i}\omega)} \tag{67}$$

$$\lim_{r\to 0} r\frac{\partial \bar{s}_c}{\partial r} = \frac{-\,Q_o}{2\,\pi\ K\,(l-d)\,(p-\mathbf{i}\omega)}\ \frac{m}{n\pi}\ \left[sin\frac{n\pi l}{m}-sin\frac{n\pi d}{m}\right] \tag{68}$$

Simplification yields:

$$\bar{s}_c(r,n,p) = \frac{Q_o}{2\,\pi\ K\,(p-\mathbf{i}\omega)}\ K_o\left[r\ \sqrt{\frac{p}{D}+\left(\frac{n\pi}{m}\right)^2}\right] \tag{69}$$

and for n=0. Using Equation (68):

$$A_{1,n} = \frac{Q_o}{2\,\pi\ K\,(l-d)\ (p-\mathbf{i}\omega)}\ \frac{m}{n\pi}\ \left[sin\frac{n\pi l}{m}-sin\frac{n\pi d}{m}\right] \tag{70}$$

Therefore:

$$\bar{s}_c(r,n,p) = \frac{Q_o}{2\,\pi\ K\,(l-d)\,(p-\mathbf{i}\omega)}\cdot \cdot\ \frac{m}{n\pi}\ \left[sin\frac{n\pi l}{m}-sin\frac{n\pi d}{m}\right]K_o\left[r\ \sqrt{\frac{p}{D}+\left(\frac{n\pi}{m}\right)^2}\right] \tag{71}$$

for n=1, 2, 3,.... The inverse Fourier cosine transform is given by:

 DOI 10.1007/s10040-003-0255-7

$$\bar{s}(r,z,p) = \frac{1}{m}\bar{s}_c(r,0,p) \; + \; \frac{2}{m}\int_{n=1}^{\infty} \bar{s}_c(r,n,p)\; cos\frac{n\pi z}{m} \tag{72}$$

Inverting Eqs. (69) and (71) yields:

$$\bar{s}(r,n,p) = \frac{Q_o}{2\,\pi\; T\,(p-\mathbf{i}\omega)}\; \left\{ K_o\left[r\,\sqrt{\frac{p}{D}+\left(\frac{n\pi}{m}\right)^2}\right] + \frac{2m}{\pi\,(l-d)}\int_{n=1}^{\infty}\; \frac{1}{n}\;\left[sin\frac{n\pi l}{m} - sin\frac{n\pi d}{m}\right] K_o\left[r\,\sqrt{\frac{p}{D}+\left(\frac{n\pi}{m}\right)^2}\right]\; cos\frac{n\pi z}{m}\right\} \tag{73}$$

Convolution can be used to obtain the inverse Laplace transform:

$$s(r,z,t) = \frac{Q}{2\pi T}[C_1 + C_2 - C_3 - C_4] \tag{74}$$

where:

$$C_1 = K_o\left[r\,\sqrt{\frac{\mathbf{i}\omega}{D}}\right] \tag{75}$$

$$C_2 = \frac{2m}{\pi(l-d)}\int_{n=1}^{\infty}\; \frac{1}{n}\;\left[sin\frac{n\pi l}{m} - sin\frac{n\pi d}{m}\right] K_o\left[r\,\sqrt{\frac{\mathbf{i}\omega}{D}+\left(\frac{n\pi}{m}\right)^2}\right]\; cos\frac{n\pi z}{m} \tag{76}$$

$$C_3 = \int_o^{\infty}\frac{\lambda J_o(r\lambda)}{\frac{\mathbf{i}\omega}{D}+\lambda^2}\; e^{-(\mathbf{i}\omega + D\lambda^2)t}\; d\lambda \tag{77}$$

$$C_4 = \frac{2m}{\pi(l-d)}\int_{n=1}^{\infty}\; \frac{1}{n}\;\left[sin\frac{n\pi l}{m} - sin\frac{n\pi d}{m}\right] cos\frac{n\pi z}{m}\; \int_o^{\infty}\frac{\lambda J_o(r\lambda)}{\frac{\mathbf{i}\omega}{D}+\lambda^2+\left[\frac{n\pi}{m}\right]^2}\; e^{-\left(\mathbf{i}\omega + D\lambda^2 + \left[\frac{n\pi D}{m}\right]^2\right)t}\; d\lambda \tag{78}$$

The integral terms in C_3 and C_4 are transient responses to initial conditions. The steady periodic response is, therefore:

$$s(r,z,t) = \frac{Q}{2\,\pi\; T}\;[C_1 + C_2] \tag{79}$$

The steady periodic response in an observation well screened from a depth of l' to d' is the average value of the drawdown over that interval, and is given by:

$$s(r,l',d',t) = \frac{Q}{2\,\pi\; T\,(l'-d')}\;\int_{d'}^{l'}\;[C_1 + C_2]\; dz \tag{80}$$

which is equal to:

$$s(r,l',d',t) = \frac{Q}{2\pi T}\;\left\{ K_o\left[r\,\sqrt{\frac{\mathbf{i}\omega}{D}}\right] + \frac{2m^2}{\pi^2\;(d'-l')\;(l-d)}\cdot\int_{n=1}^{\infty}\;\frac{1}{n^2}\left[sin\frac{n\pi l}{m} - sin\frac{n\pi d}{m}\right] K_o\left[r\,\sqrt{\frac{\mathbf{i}\omega}{D}+\left(\frac{n\pi}{m}\right)^2}\right]\left[sin\frac{n\pi l'}{m} - sin\frac{n\pi d'}{m}\right]\right\} \tag{81}$$

References

Aadland RK, Gellici JA, Thayer PA (1995) Hydrogeologic framework of west-central South Carolina. Rep 5. South Carolina Department of Natural Resources, Water Resources Division, Columbia

Barker JA (1988) A generalized radial flow model for hydraulic tests in fractured rock. Water Resour Res 24(10):1796–1804

Black JH, Kipp KL Jr (1981) Determination of hydrogeological parameters using sinusoidal pressure tests: a theoretical appraisal. Water Resour Res 17(3):686–692

Bruggeman GA (1999) Analytical solutions of geohydrological problems. Elsevier, New York

Carslaw HS, Jaeger JC (1953) Operational methods in applied mathematics. Oxford University Press, Oxford

Cheney W, Kincaid D (1994) Numerical mathematics and computing. Brooks-Cole, Pacific Grove, California

Ferris JG (1963) Cyclic water-level fluctuations as a basis for determining aquifer transmissibility. In: Bentall R (ed) Methods of determining permeability, transmissibility and drawdown. US Geol Surv Water-Supply Pap 1536-I:305–323

Gelhar LW (1974) Stochastic analysis of phreatic aquifers. Water Resour Res 10(3):539–545

Haborak KG (1999) Analytical solutions to flow in aquifers during sinusoidal aquifer pump tests. MS Thesis, University of Georgia, Athens, Georgia

Hantush MS (1964) Hydraulics of wells. In: Chow VT (ed) Advances in hydroscience, vol 1. Academic Press, New York, pp 281–432

Hantush MS, Jacob CE (1955) Non-steady radial flow in an infinite leaky aquifer. Am Geophys Un Trans 36(1):95–100

Hsieh PA, Bredehoeft JD, Farr JM (1987) Determination of aquifer transmissivity from earth tide analysis. Water Resour Res 23(10):1824–1832

Mehnert E, Valocchi AJ, Heidari M, Kapoor SG, Kumar P (1999) Estimating transmissivity from the water level fluctuations of a sinusoidally forced well. Ground Water 37(6):855–860

Miles JW (1971) Integral transforms in applied mathematics. Cambridge University Press, Cambridge

Pinkus A, Zafrany S (1977) Fourier series and integral transforms. Cambridge University Press, Cambridge

Poularikas AD (1996) The transforms and applications handbook. CRC Press, Boca Raton, Florida

Rasmussen TC, Crawford LA (1997) Identifying and removing barometric pressure effects in confined and unconfined aquifers. Ground Water 35(3):502–511

Ritzi RW, Sorooshian S, Hsieh PA (1991) The estimation of fluid-flow properties from the response of water levels in wells to the combined atmospheric and earth tide forces. Water Resour Res 27(5):883–893

Rojstaczer S (1988) Determination of fluid flow properties from the response of water levels in wells to atmospheric loading. Water Resour Res 24(11):1927–1938

Rojstaczer S, Riley FS (1990) Response of the water level in a well to earth tides and atmospheric loading under unconfined conditions. Water Resour Res 26(8):1803–1817

 DOI 10.1007/s10040-003-0255-7

Saff EB, Snider AD (1993) Fundamentals of complex analysis for mathematics, science, and engineering, Prentice-Hall, New Jersey

Segerlind LJ (1984) Applied finite element analysis. Wiley, New York

Sneddon IH (1972) The use of integral transforms. McGraw-Hill, New York

Theis CV (1935) The relation between the lowering of the piezometric surface and the rate and duration of discharge of a well using ground-water storage. Am Geophys Un Trans 16:519–524

Young MH, Rasmussen TC, Lyons FC, Pennell KD (2002) Optimized system to improve pumping rate stability during aquifer tests. Ground Water 40(6):629–637

Westinghouse Savannah River Corporation (1999) Aquifer testing results from the burial ground complex (U). Book 1 of 2, Southwest Plume Test Pad, WSRC-RP-99-4069. WSRC, Aiken, South Carolina

 DOI 10.1007/s10040-003-0255-7

Estimating aquifer hydraulic properties using sinusoidal pumping at the Savannah River site, South Carolina, USA

Rasmussen, Todd C.; Haborak, Kevin G.; Young, Michael H.

01 Tanmoy Das Page 1
5/2/2019 7:39

02 Tanmoy Das Page 1
5/2/2019 7:39

03 Tanmoy Das Page 1
5/2/2019 7:39

04 Tanmoy Das Page 2
5/2/2019 12:32

05 Tanmoy Das Page 2
15/2/2019 17:57

06 Tanmoy Das Page 2
5/2/2019 12:32

07 Tanmoy Das Page 3
5/2/2019 12:32

08 Tanmoy Das Page 3
5/2/2019 12:32
hydraulic diffusivity=kb/S, k=hydraulic conductivity, b=thickness of confined aquifer, S=storage coefficient

09 Tanmoy Das Page 3
5/2/2019 12:32

10 Tanmoy Das Page 3

5/2/2019 12:40

Initial condition; not required for derivation

11 Tanmoy Das Page 3

5/2/2019 12:40

12 Tanmoy Das Page 3

5/2/2019 12:40

Boundary condition of drawdown at infi□nity

13 Tanmoy Das Page 3

5/2/2019 12:40

14 Tanmoy Das Page 3

5/2/2019 12:40

Boundary condition at periodic line source

15 Tanmoy Das Page 3

5/2/2019 12:40

16 Tanmoy Das Page 3

5/2/2019 12:32

hydraulic diffusivity=kb/S, k=hydraulic conductivity, b=thickness of confined aquifer, S=storage coefficient

17 Tanmoy Das Page 3

5/2/2019 12:32

18 Tanmoy Das Page 3

5/2/2019 12:32

hydraulic diffusivity=k/S_s

19 Tanmoy Das Page 3

5/2/2019 12:32

20 Tanmoy Das Page 3

5/2/2019 12:07

21 Tanmoy Das Page 3

5/2/2019 7:39

22 Tanmoy Das Page 3

5/2/2019 12:07

Different analytical solutions of different authors are given

23 Tanmoy Das Page 3

5/2/2019 7:39

24 Tanmoy Das Page 3

5/2/2019 15:28

http://tutorial.math.lamar.edu/Extras/ComplexPrimer/Forms.aspx

25 Tanmoy Das Page 3

5/2/2019 15:28

26 Tanmoy Das Page 9

5/2/2019 17:44

Here Q_1 and Q_2 ,are constant, has to be determined fom best from fitted sinusoidal curve, so that Q1 coswt +Q2 sin wt = Qo e(iwt+phi), phi=phase lag

27 Tanmoy Das Page 9

5/2/2019 17:44

the function is similiar to least squares functions

28 Tanmoy Das Page 9

5/2/2019 17:44

29 Tanmoy Das Page 9

5/2/2019 17:44

30 Tanmoy Das Page 9

5/2/2019 17:44

31 Tanmoy Das Page 14

26/3/2019 16:04

Bessel function : old page 103 , New 173

32 Tanmoy Das Page 14

26/3/2019 16:04

33 Tanmoy Das Page 14

26/3/2019 16:04

34 Tanmoy Das Page 14

5/2/2019 12:07

35 Tanmoy Das Page 14

15/10/2019 7:32

36 Tanmoy Das Page 14

5/2/2019 12:07